Episodic particle flux: a sampling artifact?

Meg Estapa[1], Melissa Omand[2], Colleen Durkin[3]

[1] Skidmore College, Saratoga Springs, NY
[2] University of Rhode Island, Narragansett, RI
[3] Moss Landing Marine Laboratory, Moss Landing, CA

Introduction

The distribution of sinking particle flux in time and space may reflect the patchiness of processes that contribute to the biological carbon pump. However, characterizing the true, spatiotemporal variability in particle flux is complicated by the different sampling scales of observational technologies. We show data from several recent studies that illustrate how the measured variability in particle flux is influenced by the sampling scale and the size distribution of sinking particles. During winter 2017 in the California Current, an upward-looking time-lapse camera mounted beneath a sediment trap with a 72 mm diameter gel collector was co-deployed alongside a transmissometer used as an optical sediment trap (OST), with sampling beam cross-section of ~ 7 mm. A timeseries of cumulative particle area flux subsampled from the camera images qualitatively resembles the optical attenuance flux timeseries from the transmissometer, suggesting that time variability in optical attenuance flux measured over the beam area reflects the arrival of large, rare particles. For a given flux size distribution, we show that there is an optimal minimum sampling area that will capture the 'true' flux timeseries for this size distribution.

We test this idea using data collected during the 2019 EXPORTS campaign in the North Pacific, using the variance-to-mean ratio of particle attenuance (or cross-sectional area) flux as a measure of flux variability. We compare observations collected using subsampled gel traps and co-deployed OSTs at different times during the course of the month-long cruise to determine whether these methods are sufficient to identify periods of true episodicity in the biological pump.
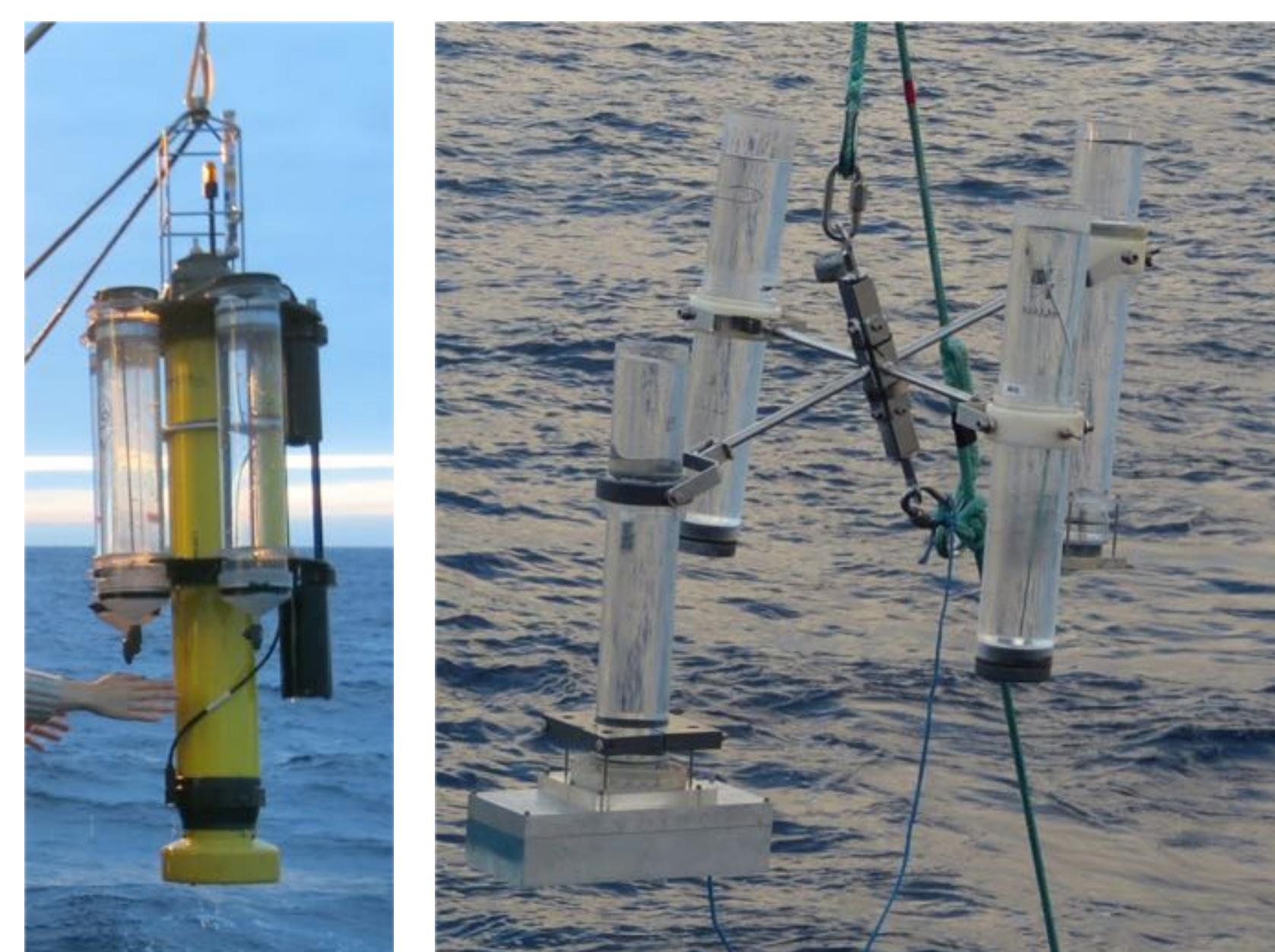

Figure 1: Field platforms. Left: Neutrally-buoyant sediment trap (NBST) carrying transmissometer that serves as an optical sediment trap (OST) and also a polyacrylamide gel collector in the base of one of the trap tubes. Right: Surface tethered array of particle interceptor tubes carrying polyacrylamide gels and also an upward-looking iPhone camera (in aluminum housing beneath front left tube).

Figure 2: Size distribution slope profiles from 2018 EXPORTS study. Power-law slopes for sinking particle size distributions determined from gel traps showed a depth dependence. The importance of large particles generally decreased with depth except at 330 m. This dependence was the same throughout the EXPORTS study. Figure shows PSD slopes from NBST gels except surface tethered trap array (STT) gels (squares) were included at 330 m on 17-Aug, and 500 m on all dates, where NBST samples (circles) weren't available. Error bars show uncertainty in PSD slope arising from Monte Carlo propagation of particle counting uncertainty.
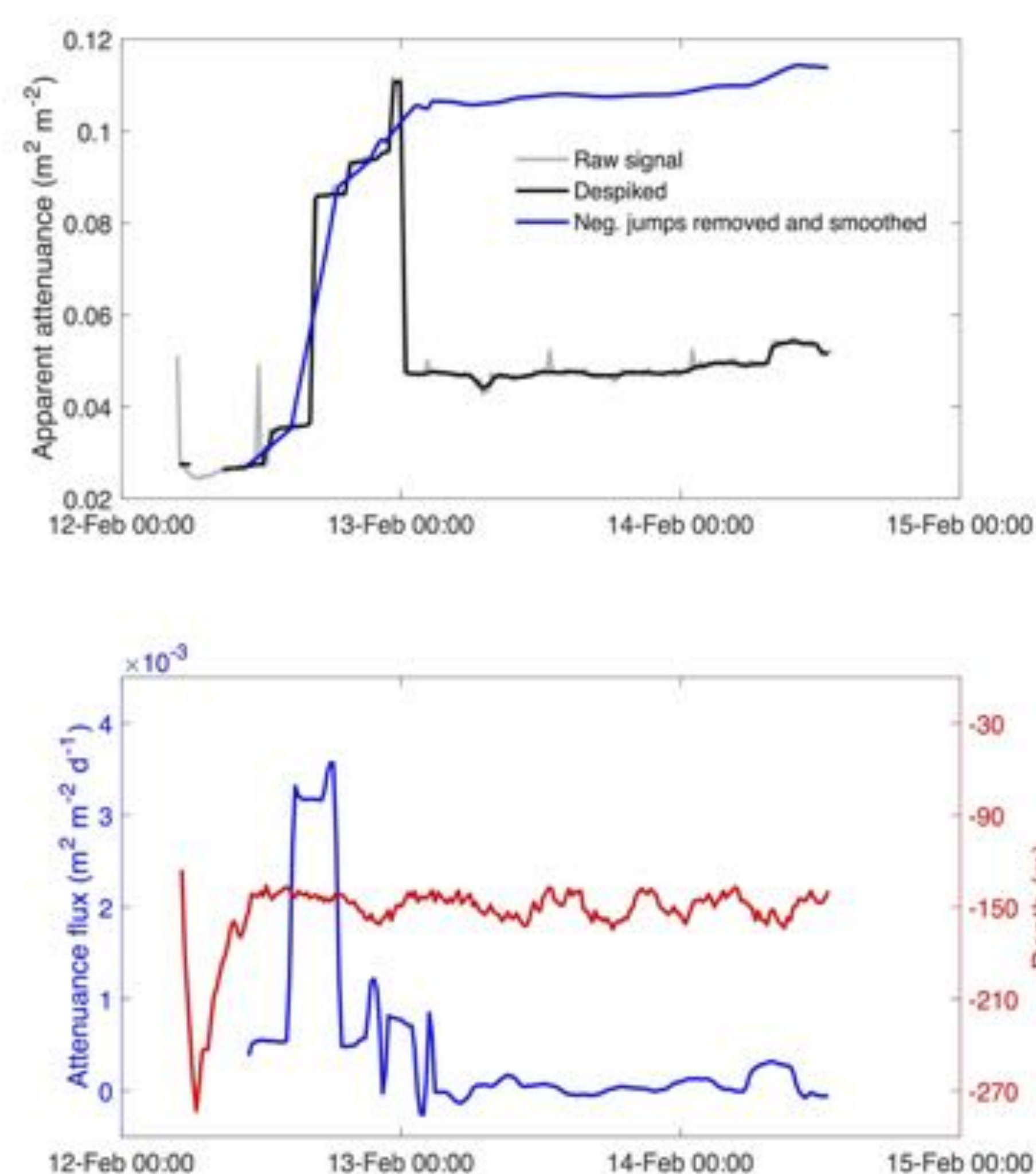

Figure 3: Optical sediment trap method. Data shown were collected in the California Current during February 2017 aboard the R/V Falkor. Upper panel: Data processing steps to yield OST flux proxy. Raw signal (gray line) is despiked with a median filter (black line), and then rapid downward "jumps" are removed and the signal smoothed through a 4-hour running mean filter (blue line). Bottom panel: The gradient with respect to time of the smoothed, despiked signal (blue line, left y-axis) is the time-resolved proxy for sinking particle flux. The platform depth is also shown (red line, right y-axis)
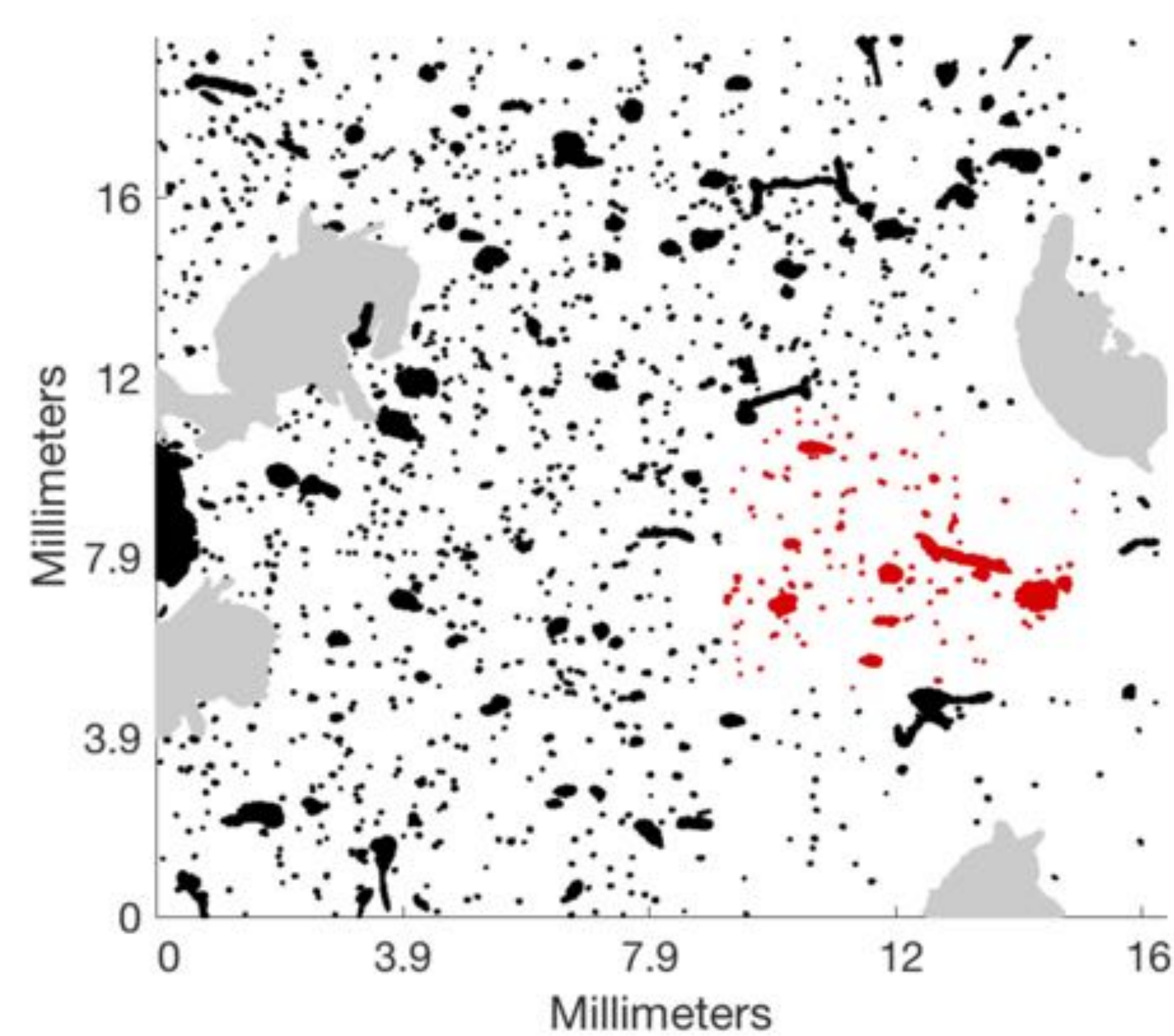

Figure 4. Left) The final processed image from a sediment trap camera below a gel sediment trap that was deployed at 130m for 62 hours in the California Current during February 2017 on the RV Falkor. The largest particles (>300 um) shown in white, were identified though image contouring. The red circles indicate the various diameters of the 'beam' that were used in a Monte Carlo analysis to determine the optimal beam diameter for this sample. We tested 0.67 cm (nominally the OST beam size), 1.3 cm, 2.7 cm and 5 cm. Right) Time-series of the fractional area covered by the >300um particle class in the gel sediment trap at Station M (thick black line). The particle images in the 76 mm diameter gel cup were identified and tracked over time. If they drifted from their initial position, they were pinned back to that position. Then, a sub-region of the entire image was defined (0.7, 1.3, 2.7 and 5 mm diameter) and randomly placed at 10 locations each within the full image. The particles arriving within these sub-regions were sampled as independent time-series (thin colored lines) demonstrating the role that arrivals of discrete large particles can play in setting the time-resolved flux variability. This role is enhanced as the sampled region gets smaller. And as it is increased, the individual time-series begin to converge with the total. The thick black dashed line is the mean of the 10 realizations, and the shaded gray region is the standard deviation in each case.

Figure 5. Gel particle size distribution example. The image above was collected during the EXPORTS North Pacific field campaign in August 2018 at Station Papa. A single field of view (7.7 um/pixel) is shown as an example; typically 16 fields of view at this magnification are collected for each sediment trap sample. The image shows particle cross sections identified via an edge-detection algorithm (background is white; see C.A. Durkin's poster for more details). Gray particles were tagged as probable swimmers and were not counted. Red particles are part of a subsample with area equivalent to the OST beam cross-section.
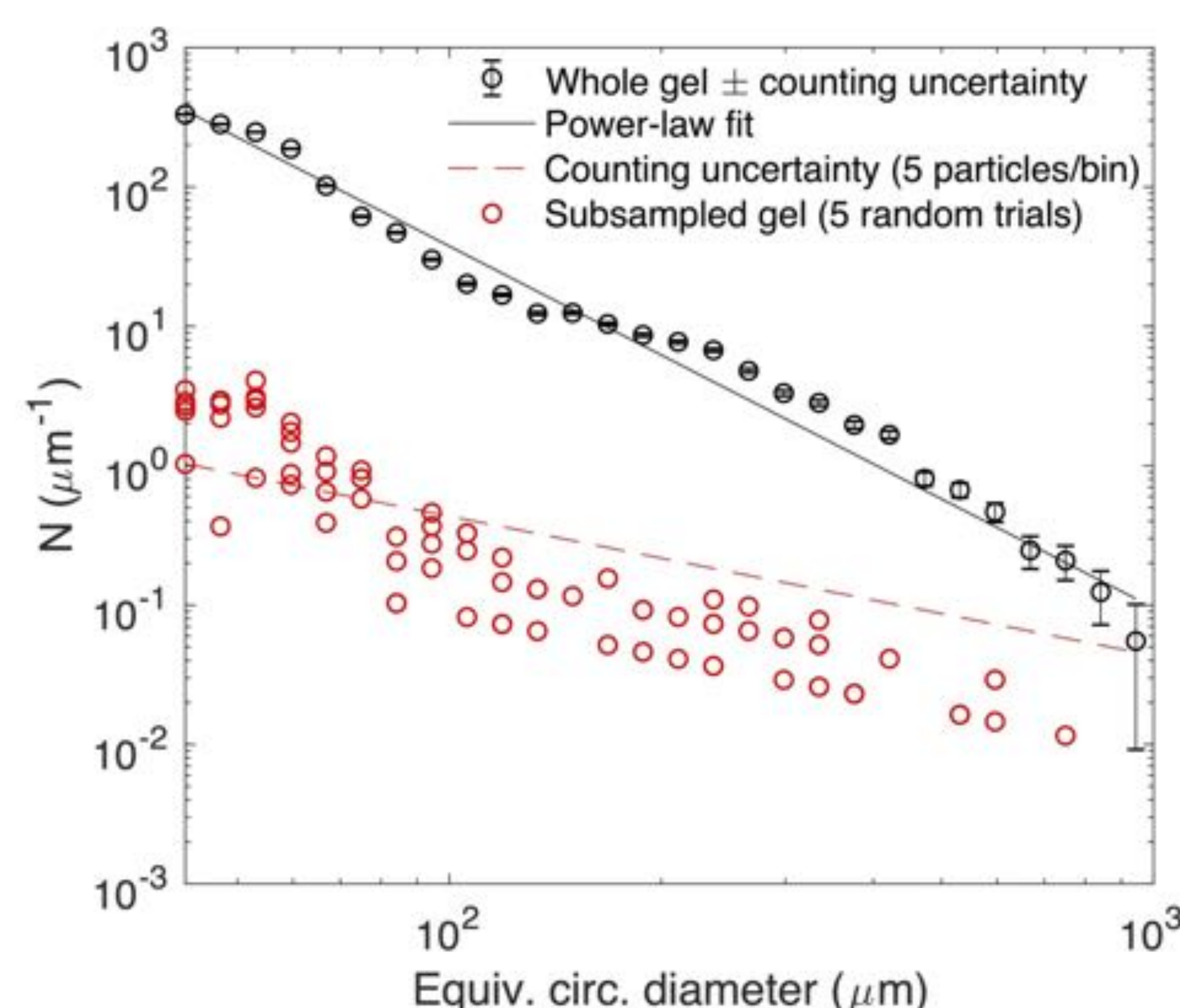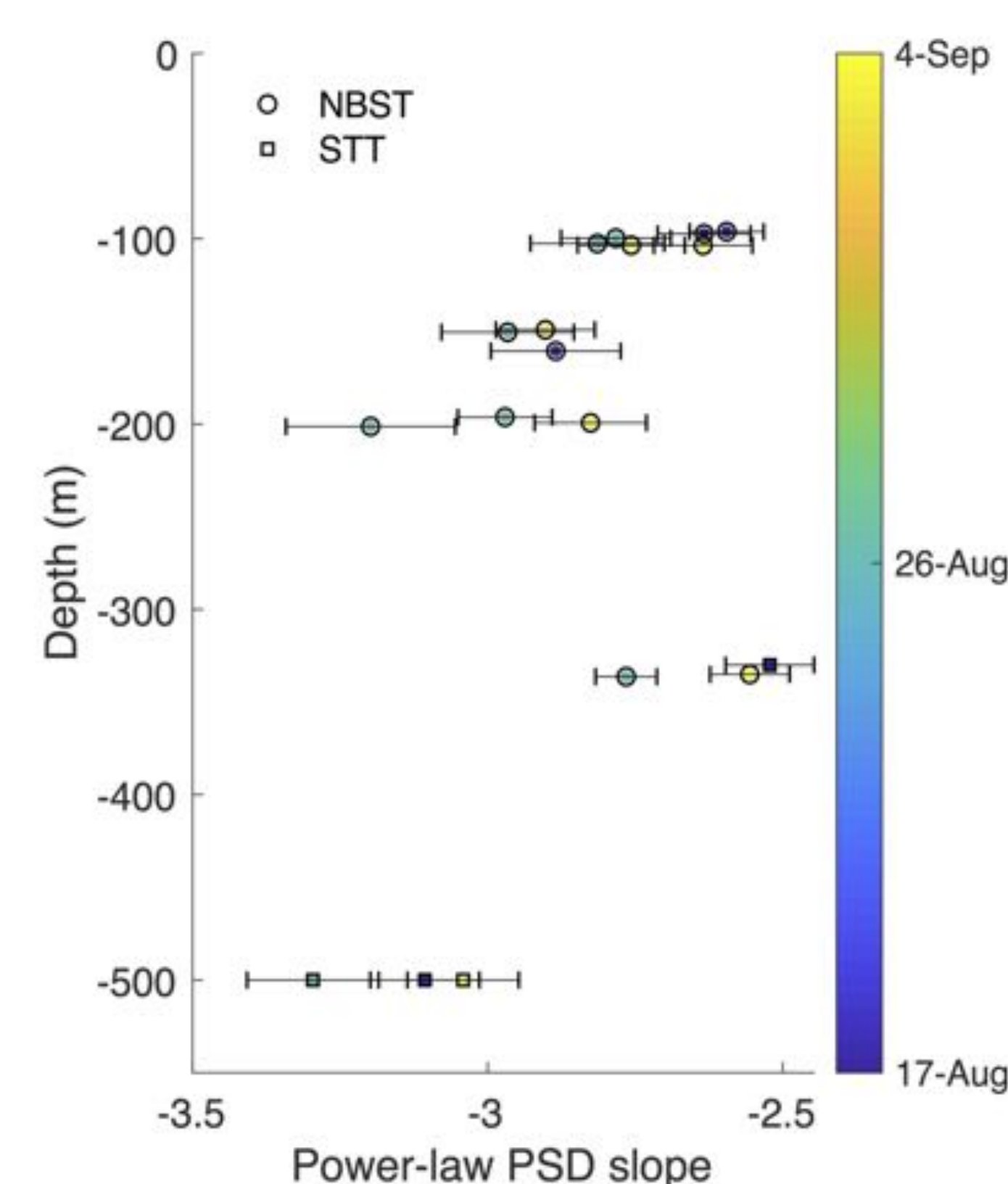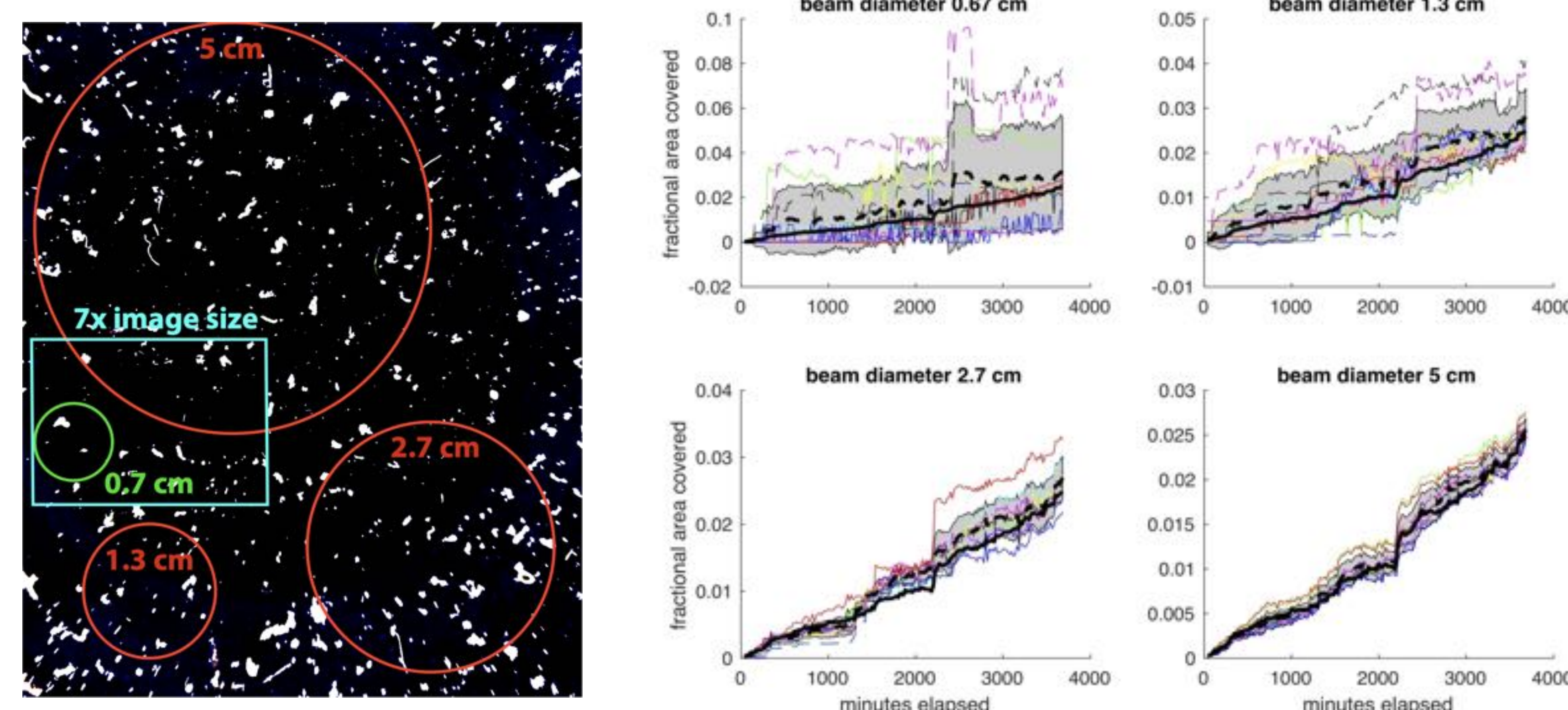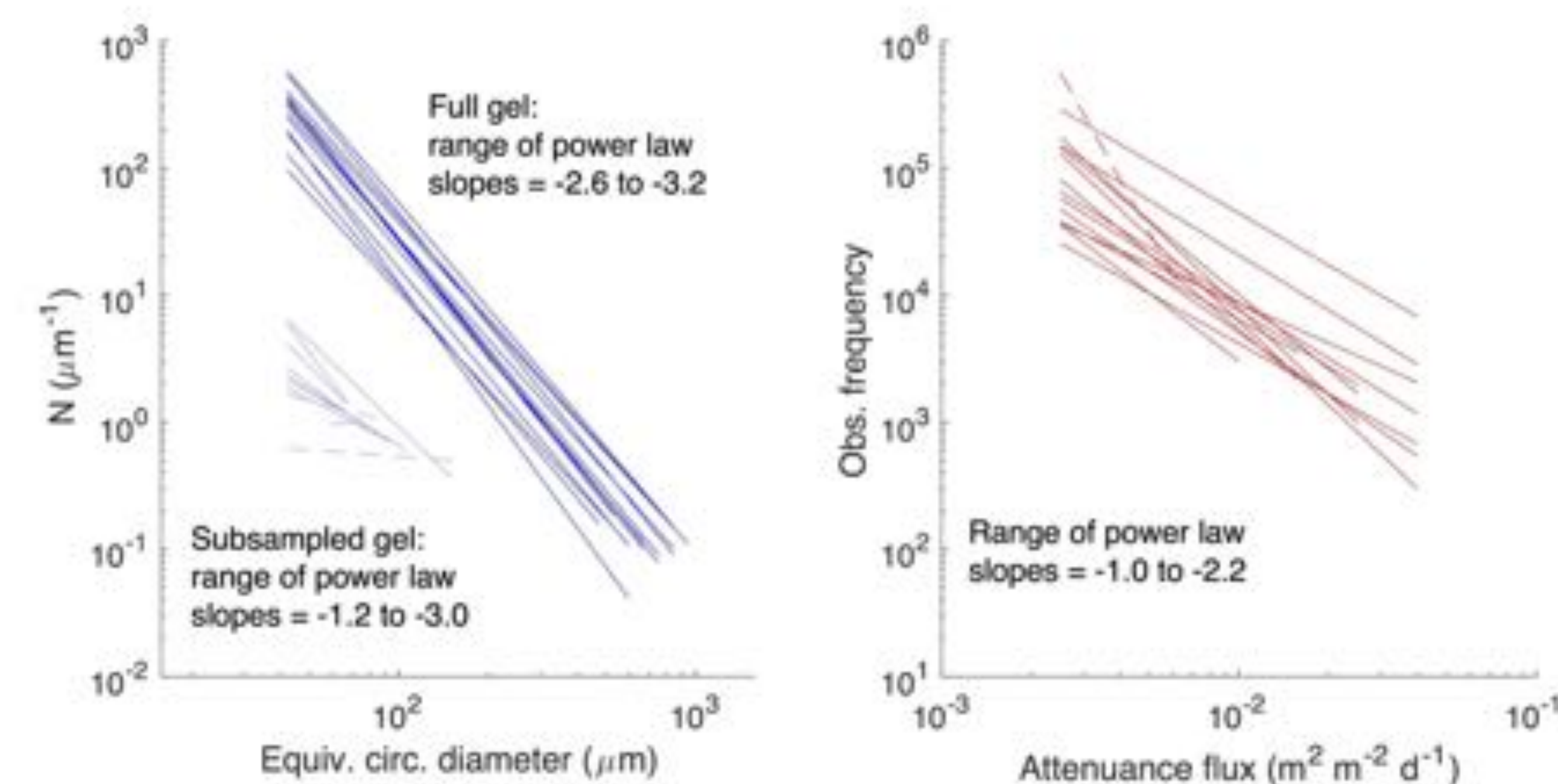

Figure 6: Particle size distribution modeling example. Data shown are from EXPORTS 2018 and correspond to Figure 5. All particles in the entire gel sample were binned by equivalent circular diameter (ECD) into log-spaced bins, and then counts were normalized by the bin width (black circles). Error bars show counting uncertainty, defined as 5 particles/bin. A power-law function of form $N(D) = A(D_0)(D/D_0)^{-S}$ was fit to the binned particle number flux distribution (black line). The size distribution of particles in randomly subsampled areas of the gel equivalent to the OST beam cross section (red circles) was measured 5 times. In most cases the subsampled particle counts were below the counting uncertainty (red dashed line) for bins larger than 70 um.

Figure 7. Power law slopes fit to binned particle number fluxes in gels (left), and to OST attenuance flux observation frequency (right). Lines are plotted only over well-sampled bins used in power-law slope fitting. Some samples were poorly described by a power law distribution (dashed lines) and are excluded from the slope ranges noted on the graphs. The slopes computed over entire gel samples (left panel, dark blue lines) are steeper and consistent with literature observations for sinking particles. The slopes computed for subsampled gels (left panel, light blue lines) and OST timeseries (right panel) are flatter, consistent with undersampling of large particle size classes and exclusion of undercounted bins from the power-law fit.

Conclusions

- Particle size distribution slopes in gel sediment traps from the EXPORTS North Pacific field campaign show that sinking particle size varies with depth and may reflect processes that repackage or produce particles at depth.
- A timeseries of particle accumulation from the subsampled time-lapse imagery shows qualitative similarity to large steps in the OST data, suggesting that OST 'events' may be discrete large particle arrivals.
- Spatial subsampling of sediment trap time-lapse imagery from the productive California Current shows that a detector diameter of 5 cm adequately samples most sinking material.
- Spatial subsampling of particles imaged in gel sediment traps shows that a 7 mm diameter beam may undersample larger particle size classes, resulting in apparently "flatter" power-law particle size distributions.
- If a power-law function does not adequately describe the particle size distribution at all sizes, then undersampling in any part of the size spectrum (e.g., undercounting large particles or poorly-resolving small ones) will bias the PSD slope parameter.
- While one should exercise caution in equating temporal variability in OST attenuance flux with the variability in sinking particle size distribution, the flattened power-law spectra of OST time records are consistent with the flattened PSD spectra of particles in small-area subsamples of gels.